Acta Crystallographica Section B
Structural Science
ISSN 0108-7681

Tautomerism and hydrogen bonding in guaninium phosphite and guaninium phosphate salts

El-Eulmi Bendeif,[a] Slimane Dahaoui,[a] Nourredine Benali-Cherif[b] and Claude Lecomte[a]*

[a]Laboratoire de Cristallographie et Modélisation des Matériaux Minéraux et Biologiques LCM^{3}B CNRS UMR 7036, Université Henri Poincaré, Nancy 1, Faculté des Sciences, BP 239, 54506 Vandoeuvre-lès-Nancy CEDEX, France, and [b]Institut des Sciences Exactes, Technologie et Informatique Centre Universitaire de Khenchela, Khenchela 40000, Algeria

Correspondence e-mail: claude.lecomte@lcm3b.uhp-nancy.fr

Received 6 October 2006
Accepted 31 January 2007

The crystal structures of three similar guaninium salts, guaninium monohydrogenphosphite monohydrate, $C_5H_6N_5O^+\cdot H_2O_3P^-\cdot H_2O$, guaninium monohydrogenphosphite dihydrate, $C_5H_6N_5O^+\cdot H_2O_3P^-\cdot 2H_2O$, and guaninium dihydrogenmonophosphate monohydrate, $C_5H_6N_5O^+\cdot H_2O_4P^-\cdot H_2O$, are described and compared. The crystal structures have been determined from accurate single-crystal X-ray data sets collected at 100 (2) K. The two phosphite salts are monoclinic, space group $P2_1/c$, with different packing and the monophosphate salt is also monoclinic, space group $P2_1/n$. An investigation of the hydrogen-bond network in these guaninium salts reveals the existence of two ketoamine tautomers, the N9H form and an N7H form.

1. Introduction

Under physiological conditions the purine base guanine exists predominantly in the neutral, keto tautomeric form. It has long been postulated that the presence of unpreferred or rare tautomeric forms might be involved in base mispair formation during polymerase-mediated DNA replication, resulting in genetic mutations (Yun *et al.*, 2003). However, it has also been estimated that these unpreferred tautomeric forms might be present, under physiological conditions, at a very low frequency of 10^{-6} to 10^{-5} (Topal & Fresco, 1976). The complex network of hydrogen-bond interactions that modulate DNA base recognition is based on the assumption of specific tautomeric and ionic states for the nucleic acid bases. The importance of tautomeric equilibria has been widely recognized since the early work of Watson & Crick (1953). Several models of spontaneous mutation in DNA are based on the existence of minor tautomeric forms (Kwiatkowski & Pullman, 1975; Topal & Fresco, 1976; Cohen *et al.*, 2003; Slósarek *et al.*, 2006; Guille & Clegg, 2006). In the Watson–Crick base-pairing scheme of nucleic acids, the nucleic acid bases are assumed to have the amino or the lactam structure (see Fig. 1). Although it has been suggested that the purine and pyrimidine bases can also exist in their minor tautomeric imino and lactim forms (Wong, 1973), the fraction of the minor tautomers, as determined by IR, UV and thermodynamic measurements, is very small, typically less than 1% (Kenner *et al.*, 1955; Katritzky & Waring, 1963; Brown & Hewlins, 1968; Wolfenden, 1969; Schweizer & Hollis, 1969; Kokko *et al.*, 1962; Miles *et al.*, 1963; Becker *et al.*, 1965). However, ^{1}H NMR results have indicated that the minor tautomers of cytosine and guanine are present to 15% at room temperatures in neutral aqueous solution (Lee *et al.*, 1971, 1972; Lee & Chan, 1972; Chan & Lee, 1972).

This explains the great experimental and theoretical effort focused on the study of tautomerism of nucleic acid bases. Recently some theoretical studies have been conduced on the tautomerism of neutral guanine (Colominas *et al.*, 1996; Barsky & Colvin, 2000; Choi & Miller, 2006). It was found that neutral guanine exists in the aqueous phase as a mixture of two major ketoamine tautomers, the N9H form (*A*, population 85%) and a N7H form (*B*, population 15%; Fig. 2). Among these two tautomers, *B* has been shown by theoretical studies to be more stable than *A* for isolated guanine (Lin *et al.*, 1980). However, *A* was known to be the only tautomeric form found in polar solvents (Miles *et al.*, 1963; Shapiro, 1968) or in the crystalline state (Thewalt *et al.*, 1971).

Using structural data retrieved from the Cambridge Structural Database, Taylor & Kennard (1982) determined that the N7 position (*B* form) is the most favourable protonation site of the guanine molecule. They found significant changes in the geometry of the purine skeleton owing to protonation, especially in the C5—N7—C8 angle, 104.2 (3)°, in the neutral guanine molecule and 108.0 (2)° in the protonated case. Del Bene (1983) optimized the geometry of both neutral and protonated guanine molecules and calculated the protonation energies for four different protonation sites (N1, N3, N7 and N9). She came to the same conclusions as Taylor & Kennard (1982), *i.e.* the most favourable site is N7 with C5—N7—C8 angles of 104.0 and 109.1° in the neutral and the protonated guanine, respectively.

We describe the crystal structures of guaninium monohydrogenphosphite monohydrate, $C_5H_6N_5O^+\cdot H_2O_3P^-\cdot H_2O$ (I), guaninium monohydrogenphosphite dihydrate, $C_5H_6N_5O^+\cdot H_2O_3P^-\cdot 2H_2O$ (II), and guaninium dihydrogenmonophosphate monohydrate, $C_5H_6N_5O^+\cdot H_2O_4P^-\cdot H_2O$ (III). Crystals of these salts are also of interest because they serve as convenient model systems to compare the structural properties of the two tautomeric forms in the crystalline state.

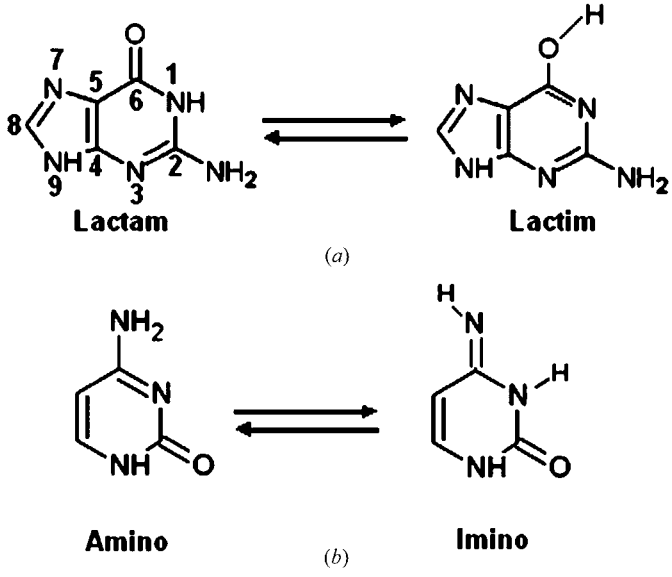

Figure 1
The tautomers of (*a*) guanine and (*b*) cytosine.

2. Experimental

2.1. Syntheses

The synthesis of (I) was carried out by dissolving the guanine base (Aldrich, 98%) in a concentrated acidic aqueous solution of H_3PO_3 (Merck, 30%). The solution was gently heated and then set aside for evaporation. Colorless single crystals of a prismatic form grew from the solution, by slow evaporation at room temperature, over a period of a few days, from which one small specimen was selected and used for X-ray analysis. Crystals of (II) were obtained by slow evaporation at room temperature of a dilute aqueous solution containing the guanine base and phosphorous acid in stoichiometric ratios. A few days later, crystals grew as white needles. Crystals of (III) were prepared by mixing two dilute aqueous solutions of guanine and orthophosphoric acid, H_3PO_4 (Carlo ERBA, 85%), so as to obtain an equimolar ratio in the resulting solution. This solution was then kept at room temperature and colorless needles appeared after a very long 9 month period.

2.2. Single-crystal X-ray diffraction

The crystal structures of the three guanine hybrid materials, *i.e.* guaninium monohydrogenphosphite monohydrate (I), guaninium monohydrogenphosphite dihydrate (II) and guaninium dihydrogenmonophosphate monohydrate (III), have been determined by single-crystal X-ray diffraction analysis. Diffraction data were collected at 100 (2) K using an Oxford–Xcalibur–Sapphire2 CCD-based diffractometer on crystals of 0.40 × 0.15 × 0.10 mm for (I), 0.40 × 0.15 × 0.10 mm for (II) and 0.42 × 0.10 × 0.07 mm for (III) with graphite-monochromated Mo $K\alpha$ radiation (λ = 0.71073 Å) equipped with a liquid-nitrogen Oxford Cryostream cooling device. The temperature control was calibrated using a K-type Chromel–Alumel thermocouple positioned at the same place on the crystal. The cell parameters were determined from an analysis of the Bragg peak positions collected on the same sets of 15 images. X-ray diffraction data were collected at a fixed detector position using ω step scans repeated at eight different values of the angle. Each frame covered a 1° omega rotation

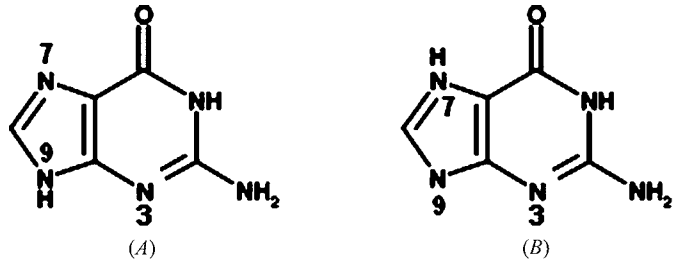

Figure 2
The two neutral guanine tautomeric forms N9H (*A*) and N7H (*B*).

Table 1
Experimental details.

	(I)	(II)	(III)
Crystal data			
Chemical formula	$C_5H_6N_5O^+\cdot H_2PO_3^-\cdot H_2O$	$C_5H_6N_5O^+\cdot H_2PO_3^-\cdot 2H_2O$	$C_5H_6N_5O^+\cdot H_2PO_4^-\cdot H_2O$
M_r	251.15	269.17	267.15
Cell setting, space group	Monoclinic, $P2_1/c$	Monoclinic, $P2_1/c$	Monoclinic, $P2_1/n$
Temperature (K)	100 (2)	100 (2)	100 (2)
a, b, c (Å)	4.9700 (2), 12.7506 (7), 15.0499 (8)	4.6812 (4), 24.0561 (15), 9.5186 (7)	4.5414 (3), 12.5774 (6), 18.1485 (9)
β (°)	92.293 (4)	99.773 (7)	93.689 (5)
V (Å^3)	952.96 (8)	1056.35 (14)	1034.48 (10)
Z	4	4	4
D_x (Mg m^{-3})	1.751	1.692	1.715
Radiation type	Mo $K\alpha$	Mo $K\alpha$	Mo $K\alpha$
μ (mm^{-1})	0.308	0.291	0.296
Crystal form, color	Needle, white	Needle, white	Needle, white
Crystal size (mm)^3	0.40 × 0.15 × 0.10	0.60 × 0.15 × 0.10	0.42 × 0.10 × 0.07
Data collection			
Diffractometer	Xcalibur-Saphire2	Xcalibur-Saphire2	Xcalibur-Saphire2
Data collection method	φ	φ	φ
Absorption correction	Integration	Integration	Integration
T_{min}	0.93	0.845	0.87
T_{max}	0.98	0.972	0.98
No. of measured, independent and observed reflections	13 648, 2749, 2727	31 247, 3086, 2911	42 941, 3013, 2971
Criterion for observed reflections	$I>2\sigma(I)$	$I>2\sigma(I)$	$I>2\sigma(I)$
R_{int}	0.0410	0.0402	0.0628
θ_{max} (°)	30.0	30.0	30.0
Intensity decay	None	None	None
Refinement			
Refinement on	F^2	F^2	F^2
$R[F^2>2\sigma(F^2)]$, $wR(F^2)$, S	0.043, 0.105, 1.15	0.040, 0.098, 1.17	0.042, 0.107, 1.11
No. of reflections	2749	3086	3013
No. of parameters	185	202	194
H-atom treatment	Mixture of independent and constrained refinement	Mixture of independent and constrained refinement	Mixture of independent and constrained refinement
Weighting scheme	$w = 1/[\sigma^2(F_o^2) + (0.0523P)^2 + 0.7658P]$, where $P = (F_o^2 + 2F_c^2)/3$	$w = 1/[\sigma^2(F_o^2) + (0.0432P)^2 + 0.8027P]$, where $P = (F_o^2 + 2F_c^2)/3$	$w = 1/[\sigma^2(F_o^2) + (0.064P)^2 + 0.5194P]$, where $P = (F_o^2 + 2F_c^2)/3$
$(\Delta/\sigma)_{max}$	0.001	< 0.0001	< 0.0001
$\Delta\rho_{max}$, $\Delta\rho_{min}$ (e Å^{-3})	0.62, −0.28	0.54, −0.27	0.54, −0.38

Computer programs used: *CrysAlis CCD* and *CrysAlis RED* (Oxford Diffraction, 2004), *SHELXS*97 and *SHELXL*97 (Sheldrick, 1997), *ORTEP*III (Farrugia, 1997), *WinGX* (Farrugia, 1999).

step. The intensity decay was monitored by repeating the initial frames at the end of the data collections and analysing the duplicate reflections. Coverage of reciprocal space was more than 99% complete to $\sin\theta/\lambda$ of 0.7 Å^{-1}. Data processing was performed using the *CrysAlis RED* program (Oxford Diffraction, 2004). Absorption effects were corrected by numerical methods based on crystal face indexing (using the program *ABSORB*; DeTitta, 1985). Equivalent reflections were scaled and averaged using *SORTAV* (Blessing, 1995). The structures were solved by direct methods (Sheldrick, 1997) and successive Fourier synthesis, and then refined by full-matrix least-squares refinements on F^2. All calculations were carried out using the *WinGX* software package (Farrugia, 1999). The electron density of the H atoms was clearly identified in the Fourier difference maps, and their atomic coordinates and isotropic displacements parameters were refined. Other details of the crystallographic and refinement data are summarized in Table 1.[1]

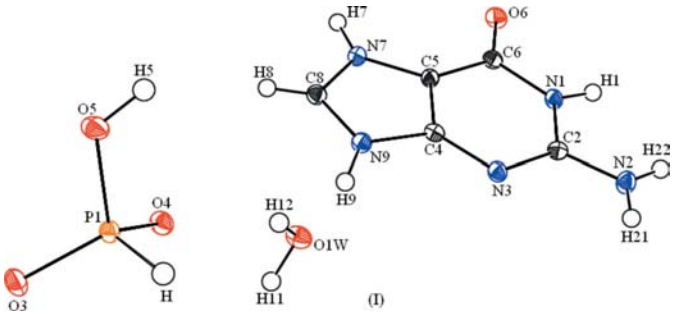

Figure 3
A perspective view of the guaninium monohydrate monohydrogenphosphite with atom-labeling scheme. Displacement ellipsoids are drawn at the 50% probability level. H atoms are represented by spheres.

[1] Supplementary data for this paper are available from the IUCr electronic archives (Reference: LB5008). Services for accessing these data are described at the back of the journal.

Table 2
Bond lengths (Å) and angles (°) for monohydrogenphosphite anions in (I) and (II) and for dihydrogenmonophosphate in (III).

(I)				
P1	**O3**	**O4**	**O5**	**H12**
O3	*1.490 (1)*	2.552 (1)	2.510 (2)	2.260 (2)
O4	115.81 (6)	*1.523 (1)*	2.523 (1)	2.252 (2)
O5	109.73 (4)	108.87 (6)	*1.579 (1)*	2.247 (2)
H	109.2 (10)	108.2 (10)	104.4 (10)	*1.26 (2)*
(II)				
P1	**O3**	**O4**	**O5**	**H12**
O3	*1.504 (1)*	2.570 (2)	2.546 (2)	2.248 (2)
O4	116.72 (6)	*1.514 (1)*	2.483 (2)	2.255 (2)
O5	111.68 (6)	107.14 (6)	*1.572 (1)*	2.272 (2)
H	107.6 (9)	108.7 (9)	104.2 (9)	*1.28 (2)*
(III)				
P1	**O1**	**O2**	**O3**	**O4**
O1	*1.5090 (9)*	2.533 (1)	2.531 (1)	2.466 (1)
O2	114.01 (6)	*1.510 (1)*	2.523 (1)	2.546 (1)
O3	110.49 (6)	109.84 (6)	*1.572 (1)*	2.485 (2)
O4	106.30 (6)	111.32 (6)	104.42 (6)	*1.573 (1)*

The P—O and P—H distances in (I) and (II), and the P—O distances in (III) run diagonally across the table (in italics). The three O—P—O angles and the three O—P—H angles in (I) and (II), and the six O—P—O angles in (III) are below the diagonal. The five internal O···O distances as well as the O···H distances in (I) and (II), and the six internal O···O distances in (III) are above the diagonal.

Table 3
Bond lengths (Å) and angles (°) for the guaninium cations.

Compound	(I)	(II)	(III)
Pyrimidine ring			
C6—N1	1.391 (2)	1.395 (2)	1.383 (2)
N1—C2	1.376 (2)	1.376 (2)	1.380 (2)
C2—N3	1.334 (2)	1.336 (2)	1.330 (2)
N3—C4	1.349 (2)	1.352 (2)	1.349 (2)
C4—C5	1.384 (2)	1.382 (2)	1.387 (2)
C5—C6	1.426 (2)	1.426 (2)	1.417 (2)
C6—O6	1.235 (2)	1.234 (2)	1.247 (2)
C2—N2	1.336 (2)	1.341 (2)	1.333 (2)
C6—N1—C2	126.0 (1)	125.7 (1)	125.2 (1)
N1—C2—N3	123.4 (1)	123.5 (1)	123.2 (1)
C2—N3—C4	112.2 (1)	112.4 (1)	113.0 (1)
N3—C4—C5	127.7 (1)	127.5 (1)	127.2 (1)
C4—C5—C6	120.0 (1)	120.3 (1)	119.5 (1)
C5—C6—N1	110.4 (1)	110.5 (1)	111.8 (1)
Imidazolyle ring			
C5—N7	1.386 (2)	1.385 (2)	1.389 (2)
N7—C8	1.327 (2)	1.326 (2)	1.321 (2)
C8—N9	1.345 (2)	1.350 (2)	1.347 (2)
N9—C4	1.376 (2)	1.382 (2)	1.376 (2)
C5—N7—C8	107.9 (1)	107.4 (1)	107.3 (1)
N7—C8—N9	110.1 (1)	110.5 (1)	111.0 (1)
C8—N9—C4	108.1 (1)	107.6 (1)	107.5 (1)
N9—C4—C5	106.8 (1)	106.6 (1)	106.7 (1)
N7—C5—C4	107.1 (1)	107.7 (1)	107.4 (1)

3. Results

3.1. Structures and crystal packing

3.1.1. Guaninium monohydrogenphosphite monohydrate, $C_5H_6N_5O^+\cdot H_2O\cdot P^-\cdot H_2O$ (I). A perspective view of (I) is given in Fig. 3. The guaninium cations, phosphite anions and water molecule build almost perpendicular layers (Fig. 4). The main feature of this stacking is the presence of centrosymmetric $(H_4P_2O_6)^{2-}$ dimers holding two layers together through strong hydrogen bonds. The guaninium entities are bonded together by two N—H···N bonds, and by four N—H···O and one O—H···O hydrogen bonds to the $H_2O_3P^-$ phosphite groups and the water molecule. Their intermolecular packing appears to be controlled by a three-dimensional network of hydrogen bonds.

The monohydrogenphosphite anion shows, as expected, a distorted tetrahedral configuration (Table 2), with a long protonated P—OH [1.5790 (1) Å] bond in agreement with that already described by Harrison (2003*a*) and Bendeif *et al.* (2005). As observed in the crystal structures of guanine picrate monohydrate and thioguanine picrate monohydrate (Bugg & Thewalt, 1975), and bisguaninium hydrogenphosphate hydrate (Low *et al.*, 1986), the guanine base is monoprotonated at the imino group of the imidazolyl portion N7 owing to the reaction with phosphorous acid, while the pyrimidine imino N3 group is not protonated. The geometrical features of the guaninium cations, $C_5H_6N_5O^+$ (Table 3), are in accordance with those previously observed in similar guaninium complexes (Bugg & Thewalt, 1975; Low *et al.*, 1986; Maixner & Zachová, 1991).

The anion behaves as both hydrogen-bond donor (through the O5 atom) and acceptor (through the O3, O4 and O5 atoms). Both O3 and O4 atoms are bifurcated hydrogen-bond acceptors *via* H1 and H22 atoms, and *via* H5 and H7 atoms, respectively, while the O5 atom acts as both a hydrogen-bond donor *via* the H5 atom and an acceptor *via* the H11 atom (Table 4). These different roles explain the significant differences between the P—O distances in the $H_2PO_3^-$ tetrahedron.

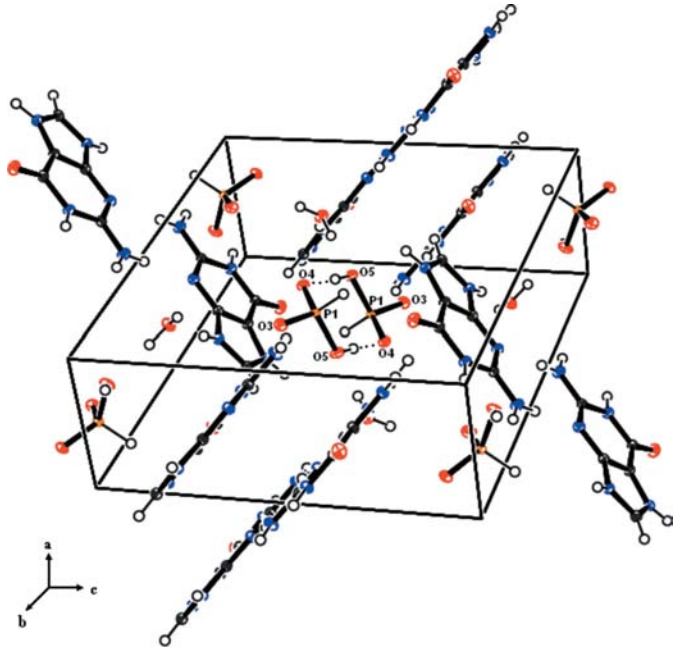

Figure 4
A perspective view of the packing of (I), showing the alternating $C_5H_6N_5O^+\cdot H_2O_3P^-$ and H_2O moieties.

These entities generate centrosymmetric $(H_4P_2O_6)_2^-$ dimers through two strong hydrogen bonds between the O4 and O5 atoms (Fig. 4).

Guaninium cations are hydrogen bonded to the anionic layers by three means: two strong hydrogen bonds (N7—H7···O4 and N1—H1···O3) and a weaker one (N2—H22···O3; Fig. 5*a*). The organic cations are laced together by only one hydrogen bond from the N2 amino group to the pyrimidine N3 imino group (N2—H21···N3) to form infinite perpendicular layers. The water molecule is involved in three strong hydrogen bonds connecting two guaninium cations *via* N9—H9···O1*W* and O1*W*—H11···O6, and one monohydrogenphosphite anion *via* O1*W*—H12···O5, so that it plays an important role in the stability of such an arrangement.

3.1.2. Guaninium monohydrogenphosphite dihydrate, $C_5H_6N_5O^+\cdot H_2O_3P^-\cdot 2H_2O$ (II). The crystal structure of (II) (Figs. 6 and 7) can be described by layers of guaninium cations, monohydrogenphosphite anions and water molecules. The asymmetric unit contains one guaninium cation, one monohydrogenphosphite anion and two water molecules. The monohydrogenphosphite chains and guaninium layers are parallel to the (001) plane and alternate at approximately $y =$

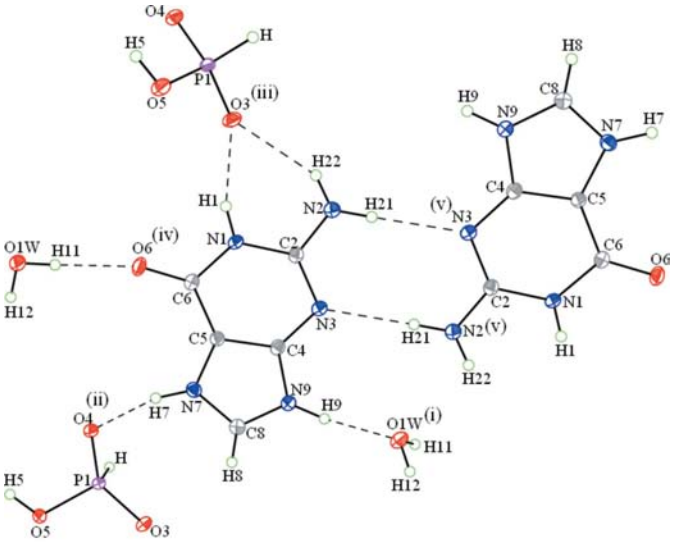

Figure 5
Hydrogen bonding involving guaninium cations (*a*) in (I) and (*b*) in (II).

Table 4
Hydrogen-bond geometry (Å, °).

D—H···A	D—H	H···A	D···A	D—H···A
(I)				
O5—H5···O4^{i}	0.88 (3)	1.66 (3)	2.535 (2)	177 (3)
N7—H7···O4^{ii}	0.92 (2)	1.80 (3)	2.698 (2)	165 (2)
N9—H9···O1*W*	0.91 (3)	1.80 (3)	2.702 (2)	170 (2)
N1—H1···O3^{iii}	0.84 (2)	1.91 (2)	2.714 (2)	160 (2)
O1*W*—H12···O5^{i}	0.88 (3)	1.88 (3)	2.755 (2)	176 (2)
O1*W*—H11···O6^{iv}	0.90 (3)	1.92 (3)	2.817 (2)	172 (3)
N2—H22···O3^{iii}	0.84 (3)	2.24 (3)	2.967 (2)	145 (2)
N2—H21···N3^{v}	0.88 (2)	2.14 (2)	3.022 (2)	178 (2)
(II)				
O5—H5···O4^{i}	0.83 (3)	1.74 (3)	2.559 (2)	173 (4)
N7—H7···O1*W*^{ii}	0.91 (3)	1.75 (3)	2.658 (2)	177 (3)
N9—H9···O3^{iii}	0.87 (2)	1.85 (2)	2.721 (2)	172 (2)
O1*W*—H11···O6^{iv}	0.79 (2)	1.95 (2)	2.730 (2)	169 (3)
N1—H1···O2*W*	0.84 (3)	1.96 (3)	2.774 (2)	164 (3)
O2*W*—H24···O3^{v}	0.82 (3)	2.00 (3)	2.814 (2)	170 (3)
O2*W*—H23···O4^{i}	0.83 (3)	2.07 (3)	2.874 (2)	164 (3)
O1*W*—H12···O4^{vi}	0.81 (3)	2.18 (3)	2.907 (2)	151 (3)
N2—H21···N3^{iii}	0.88 (2)	2.09 (2)	2.971 (2)	179 (1)
N2—H22···O3^{ii}	0.89 (2)	2.59 (2)	3.127 (2)	120 (2)
N2—H21···O2*W*^{iii}	0.89 (2)	2.38 (2)	3.130 (2)	142 (2)
(III)				
O3—H3···O1^{i}	0.90 (3)	1.67 (3)	2.567 (1)	174 (2)
O4—H4···O6^{ii}	0.85 (3)	1.75 (3)	2.592 (1)	169 (3)
N7—H7···O2^{iii}	0.92 (3)	1.74 (3)	2.651 (2)	173 (3)
N9—H9···O1*W*^{iv}	0.94 (2)	1.73 (2)	2.665 (2)	170 (2)
O1*W*—H12···O1^{v}	0.85 (3)	1.90 (3)	2.737 (1)	168 (3)
N1—H1···O2	0.90 (2)	1.85 (2)	2.751 (2)	172 (2)
O1*W*—H11···O3^{vi}	0.78 (4)	2.06 (4)	2.824 (1)	165 (3)
N2—H22···O1	0.88 (2)	1.96 (2)	2.838 (2)	175 (2)
N2—H21···N3^{vii}	0.82 (2)	2.20 (2)	3.016 (2)	178 (3)

Symmetry codes: for (I): (i) $1-x, 1-y, 1-z$; (ii) $1+x, \frac{3}{2}-y, z-\frac{1}{2}$; (iii) $x, y, z-1$; (iv) $x-1, \frac{3}{2}-y, \frac{1}{2}+z$; (v) $-x, 1-y, -z$. For (II): (i) $x, \frac{1}{2}-y, \frac{1}{2}+z$; (ii) $x, y, 1+z$; (iii) $1-x, -y, 1-z$; (iv) $-1-x, -y, 1-z$; (v) $x-1, y, z$; (vi) $-x, y-\frac{1}{2}, \frac{1}{2}-z$. For (III): (i) $1+x, y, z$; (ii) $\frac{3}{2}-x, y-\frac{1}{2}, \frac{1}{2}-z$; (iii) $\frac{3}{2}-x, \frac{1}{2}+y, \frac{1}{2}-z$; (iv) $x-1, y, z$; (v) $1-x, 1-y, 1-z$; (vi) $x, 1+y, z$; (vii) $-x, 1-y, 1-z$.

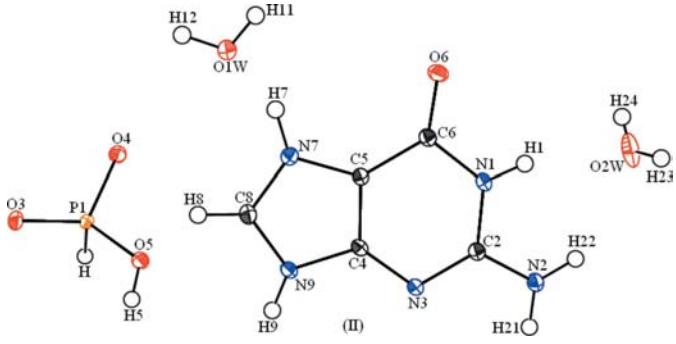

Figure 6
A perspective view of the guaninium dihydrate monohydrogenphosphite (*ORTEP*3; Farrugia, 1999) with atom-labeling scheme. Displacement ellipsoids are drawn at the 50% probability level. H atoms are represented by spheres.

$\frac{1}{4}$, $y = \frac{3}{4}$ and at $y = 0$, $y = \frac{1}{2}$, respectively (Fig. 7). The stability of such an arrangement results from a hydrogen-bond network which maintains the cohesion of the monohydrogenphosphite chains, guaninium layers and water molecules in the crystal.

Contrary to its behavior in (I), the inorganic $H_2O_3P^-$ moiety builds a zigzag polymeric network of tetrahedra, linked together by strong P—O···H—O—P hydrogen bonds along the **c** direction. Inside these infinite chains each $H_2O_3P^-$ group is connected to two adjacent neighbors by strong hydrogen bonds, O5—H5··· O4 = 2.559 (2) Å.

As in (I), the guanine base is monoproronated at N7. The geometrical features of the monohydrogenphosphite anion and of the pyrimidine and imidazolyl rings (Tables 2 and 3) are also similar to those observed in (I). Infinite layers of guaninium cations are linked to the anionic layers through two hydrogen bonds: firstly *via* a strong N9—H9···O3 hydrogen bond and secondly *via* a weaker N2—H22···O3 hydrogen bond (Fig. 5*b*). The functional groups N3 and N2 of the pyrimidine ring are a hydrogen-bond acceptor and donor, respectively, that hold together the guaninium cations through a long N3···H21—N2 hydrogen bond (Table 4). The first water molecule's O1*W* atom acts as a donor of two hydrogen bonds *via* the H11 and H12 atoms towards the O6 atom of the guaninium and O4 atom of the phosphite group, respectively, and as a hydrogen-bond acceptor *via* the H7 atom. However, the second water molecule's O2*W* atom is a donor of two hydrogen bonds to two phosphite anions *via* H24 and H23 towards O4 and O3 atoms, respectively, and a two hydrogen-bond acceptor from guaninium cations *via* H1 and H22 atoms. Therefore, the water molecules play an important role in the three-dimensional network of hydrogen bonding.

3.1.3. Guaninium dihydrogenmonophosphate monohydrate, $C_5H_6N_5O^+\cdot H_2O_4P^-\cdot H_2O$ (III). The crystal structure of (III) (Fig. 8) can be described as being composed of chains of $H_2PO_4^-$ groups extending along the **a** direction and alternating with $C_5H_6N_5O^+$ guaninium-stacked layers and water molecules. The $H_2PO_4^-$ chains are interconnected to the guaninium layers through several O···H—O and O···H—N hydrogen bonds (Fig. 8).

As expected, the distorted tetrahedral geometry of the $H_2PO_4^-$ anions (Table 2) clearly shows two main types of P—O distances: two long P—OH bonds [P—O3 1.572 (1) and P—O4 1.573 (1) Å] owing to the presence of the acidic H atoms on the PO_4 tetrahedron, and two short P—O(T) bonds [P—O1 1.5090 (9) and P—O2 1.510 (1) Å] corresponding to the

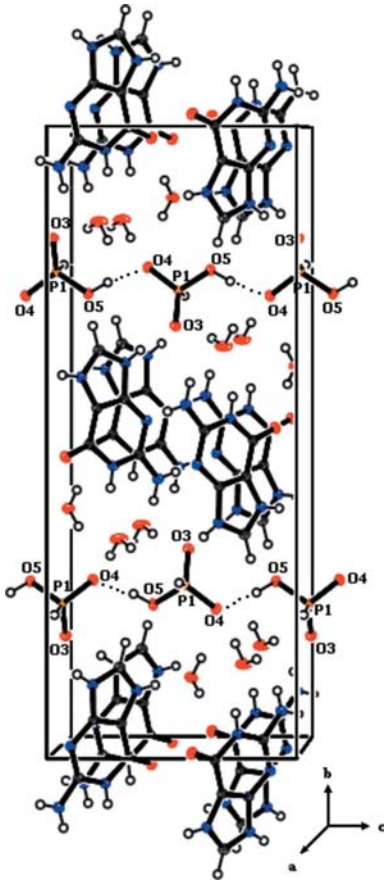

Figure 7
Unit-cell projection on the (100) plane of the packing of (II) showing the alternating $C_5H_6N_5O^+\cdot H_2O_3P^-$ and H_2O moieties.

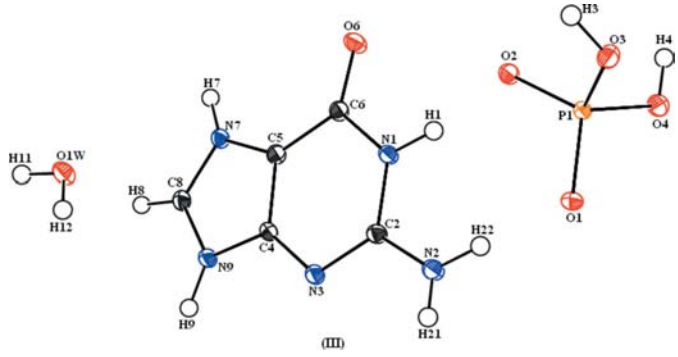

Figure 8
A perspective view of the guaninium monohydrate dihydrogen monophosphate with the atom-labeling scheme. Displacement ellipsoids are drawn at the 50% probability level. H atoms are represented by spheres.

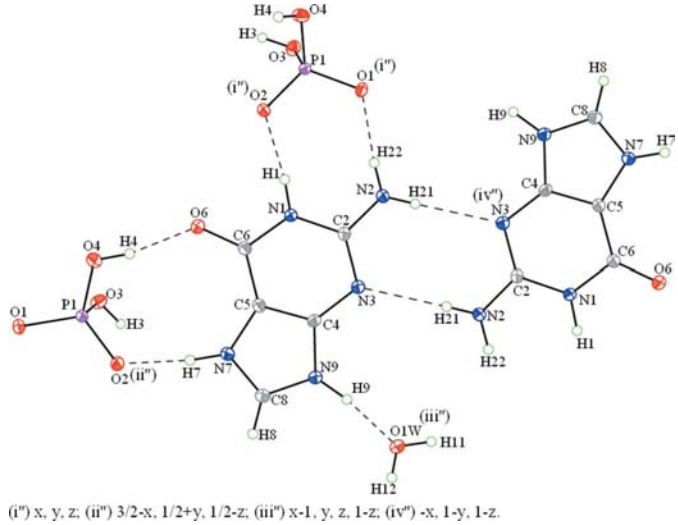

(i'') x, y, z; (ii'') 3/2-x, 1/2+y, 1/2-z; (iii'') x-1, y, z, 1-z; (iv'') -x, 1-y, 1-z.

Figure 9
Hydrogen bonding involving guaninium cations in (III).

terminal O atoms commonly observed in dihydrogen monophosphate groups (Masse & Durif, 1990; Boukhris *et al.*, 1994).

As previously observed in (I) and (II), the guanine base is also monoprotonated at the N7 imino group. The angle between the mean plane of the imidazolyl and pyrimidine rings (*i.e.* the dihedral angle) is 3.68 (2)° and this puckering along the C4—C5 bond is commonly found in purine structures (Bugg, 1972). The strong hydrogen bonds between the neighboring imino N1 atom and the amino N2 atom of the pyrimidine ring, and the $H_2PO_4^-$ anion as well as the contacts between N9 and O1*W* and N7 and $H_2PO_4^-$ are all above the average guaninium plane (Fig. 9); therefore, they prevent the two rings from being completely coplanar. The exocyclic carbonyl (O6) and amino (N2) groups deviate only slightly by 0.014 (1) and −0.008 (1) Å, respectively, from the mean least-squares plane of the purine base.

Within the inorganic chains, the $H_2PO_4^-$ tetrahedra are interconnected through a strong hydrogen bond [O3···O1 2.567 (1) Å] and form infinite chains extending along the **a** direction, with a P···P distance of 4.541 (5) Å (Fig. 10) as observed in (II) [P···P 4.814 (6) Å]. In contrast, in (I) the $H_2PO_3^-$ anions are held together in pairs yielding $H_4P_2O_6^{2-}$ dimers.

Guaninium cations are anchored to two $H_2PO_4^-$ groups belonging to two different chains by four hydrogen bonds: one $H_2PO_4^-$ anion interacts with the guaninium cation *via* strong hydrogen bonds [O4···O6 = 2.592 (1) and N7···O2 2.651 (1) Å], whereas the other $H_2PO_4^-$ anion is weakly bonded to the guaninium cation [N1···O2 2.751 (1) and N2···O1 2.838 (2) Å]. Finally, the guaninium cations are hydrogen-bonded together through a centrosymetric N2···N3 $R_2^2(8)$ ring (Fig. 9), as defined by Bernstein *et al.* (1995). These $R_2^2(8)$ rings give rise to inclined layers with an interplanar separation of 3.6105 Å; because of this long interplanar distance no layer–layer interaction was observed.

The water molecule is located in the same planes as the guanine base pairs and provides protons to form a strong hydrogen bond with $H_2PO_4^-$ groups [O1*W*···O1 2.737 (2) Å], and a relatively weaker one with another $H_2PO_4^-$ group belonging to another phosphoric chain [O1*W*···O3 2.824 (1) Å], so the water molecules ensure the connection between the phosphoric chains (Fig. 10). On the other hand, the water molecule acts as a hydrogen-bond acceptor *via* the H9 atom of the imino group containing N9 [N9···O1*W* 2.665 (1) Å].

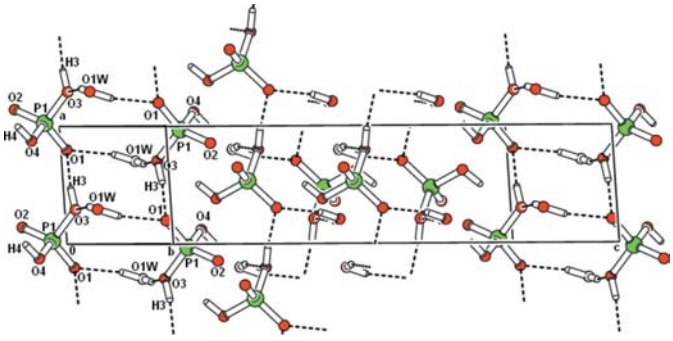

Figure 10
A perspective view of the arrangement of the monophosphate anions in (III). *PLATON* (Spek, 2003).

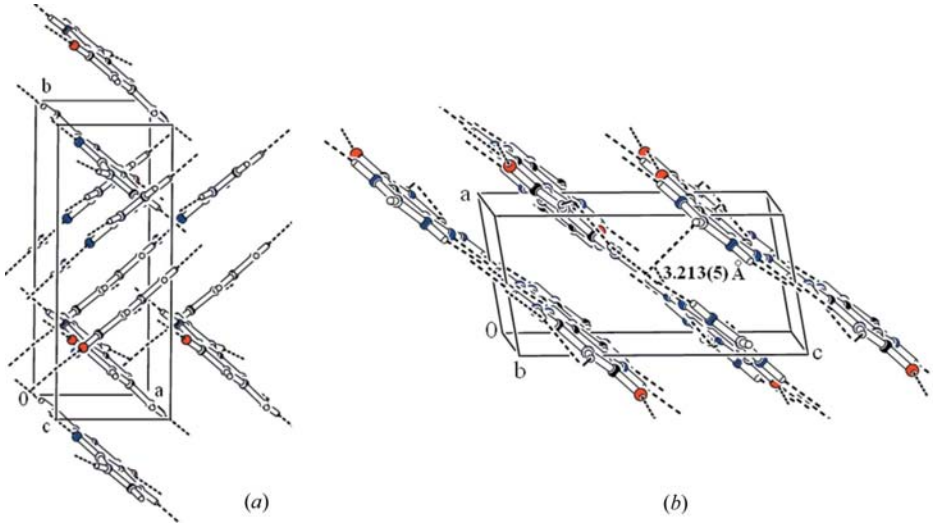

Figure 11
Guaninium arrangement (*a*) in (I) and (*b*) in (II). *PLATON* (Spek, 2003).

4. Discussion

4.1. Guaninium monohydrogenphosphite salts

4.1.1. Monohydrogenphosphite anions. The geometry around the P atom is tetrahedraly distorted in each structure: inside the $H_2PO_3^-$ tetrahedron of (I), the P—O4 bond [1.523 (1) Å] is relatively longer than the P—O3 bond [1.490 (1) Å]. This significant difference in P—O bond distances in (I) is due to the fact that O4 is involved in strong hydrogen bonding with O5 and N7 [O5···O4 2.535 (2) and N7··· O4 2.698 (2) Å] compared with O3 which is bonded *via* a weaker hydrogen bond to the N1 atom of the pyrimidine ring [N1···O3 2.714 (2) Å] and compared with the amino group N2 atom [N2···O3 2.967 (2) Å]. In (I) each $H_2PO_3^-$ tetrahedron is linked to an equivalent one by inversion symmetry through two strong hydrogen bonds between O4 and O5 atoms. This type of aggregation gives rise to strongly bonded dimers of $(H_4P_2O_6)^{2-}$ characterized by the short intermolecular O5···O4 distances [2.535 (1) Å] between the $H_2PO_3^-$ units, which are of the same order of magnitude as the O··· O distances in the tetra-

hedral unit. The internal P1···P1 distance is 4.139 (5) Å. Similar inter-anion linkages have been seen in other related organic phosphite structures, such as 2A5NP$^+$·$H_2PO_3^-$ (Pecaut & Bagieu-Beucher, 1993), $C_6H_8N^+$·$H_2PO_3^-$ (Paixão *et al.*, 2000) and $C_7H_8NO_2^+$·$H_2PO_3^-$ (Bendeif *et al.*, 2005).

By contrast, in (II) $H_2PO_3^-$ units are linked into a polymeric chain by P—O—H···O—P hydrogen bonds in the [001] direction, resulting in a P1···P1 separation of 4.814 (6) Å. The presence of such an arrangement has already been noticed in related ionic compounds, such as $CH_6N_3^+$·$H_2PO_3^-$ (Harrison, 2003*b*), $C_2H_6NO_2^+$·$H_2PO_3^-$ and $C_4H_9N_2O_3^+$·$H_2PO_3^-$ (Averbuch-Pouchot, 1993).

4.1.2. Guaninium cations. The dihedral angle between the imidazolyl and the pyrimidine rings in (I) is 2.2 (2)°, while in (II) the two rings are nearly coplanar and their deviation from the mean plane is only 0.35 (2)°. This can be explained by the strong interconnection of the guaninium cation with two $(H_4P_2O_6)^{2-}$ dimers in the *cis* conformation in (I). The deviation of the amino and carbonyl groups from the least-squares plane of pyrimidine rings is −0.068 (1), +0.018 (1) Å for (I) and of 0.052 (1), −0.025 (1) Å for (II), respectively. The delocalization of the electron density appears to be weaker in the N7—C8—N9 fragment compared with the N3—C2—N2 fragment, as shown from the interatomic distances C4—N3, N3—C2 and C2—N2 (Table 3). The shortening of the C2—N2 bond is also influenced by inter cations N2···N3 and cation–anion N2···O3 hydrogen bonds involving both H atoms of the N2 amino group. The C2—N2 bond distance is slightly longer in (II) compared with (I): the exocyclic amino group N2 atom is involved in three hydrogen bonds in (II), while in (I) only two hydrogen bonds occur (Table 4). The interplanar separation between guaninium layers in (II) is only 3.213 (5) Å (Fig. 11*b*), leading to a $\pi\cdots\pi$ stacking interaction between the base pairs, in contrast to the structure of (I) in which guaninium cations are linked together to form perpendicular layers (Fig. 11*a*). No interlayer contact is observed in such an arrangement. In conclusion, the strength of the intermolecular hydrogen-bond interactions is in agreement with the subtle intramolecular bond-length changes.

4.1.3. Hydrogen bonding. In (I) the guaninium cations are linked to the anionic layers *via* three N—H···O hydrogen bonds, N7—H7···O4, N1—H1···O3 and N2—H22···O3, while in (II) only two N—H···O hydrogen bonds occur between them, N9—H9···O3 and N2—H22···O3. The strong N7···O4 2.698 (2) Å hydrogen bond, which directly links the monohydrogenphosphite anion $H_2PO_3^-$ and the imino group N7 atom in (I) (Fig. 5*a*), leads to the suggestion that the guanine base exists in a N9H tautomeric form compared with compound (II), where the monohydrogenphosphite anion is hydrogen-bonded directly to the imino group N9 atom of the imidazolyl moiety *via* a strong hydrogen bond [N9···O3 2.721 (2) Å; Fig. 5*b*].

In the three guanine salts the guaninium cations are related together through a centrosymmetric N2···N3 $R_2^2(8)$ ring, as already observed in similar guanine compounds: guanine hydrochloride dihydrate (Iball & Wilson, 1963) and bisguaninium hydrogenphosphate hydrate (Low *et al.*, 1986), and also to that in guanine hydrochloride monohydrate (Broomhead, 1951) in which the base pairs are hydrogen-bonded together *via* centrosymmetric N7—H7···O6 bonds.

Water molecules play an important role in the three-dimensional network. They maintain the cohesion between the organic and inorganic layers in the crystal structure stacking. O1*W* plays the same role in (I) and (II), acting as a hydrogen-bond acceptor and as a double hydrogen-bond donor, while the water molecule O2*W* in (II) is a bifurcated hydrogen-bond donor and acceptor.

The hydrogen-bonding schemes for (I) and (III), although similar, exhibit slight differences in hydrogen-bond lengths (Table 4). The major differences occur in the hydrogen bonds involving the water molecule. Indeed, in (I) the water molecule is connected to one $H_2PO_3^-$ group and to the carbonyl group (O6) of the guanine base, whereas in (III) it is connected to two different $H_2PO_4^-$ groups belonging to two parallel phosphoric chains.

As also observed previously (Doran *et al.*, 2001; Harrison, 2001) the phosphite H atom is not involved in the hydrogen-bonding scheme since it is slightly negatively charged (Bendeif, 2007).

4.2. Cambridge Structural Database

A Cambridge Structural Database (CSD Version 5.27, November 2005; Allen, 2002) search revealed only nine organic–inorganic guaninium salts, which are listed in Tables 5 and 6. All the crystals are centrosymetric, most are monoclinic (seven entries), with one compound triclinic ($P\bar{1}$) and one orthorhombic (*Pnma*). Guanine cations are divided into three categories, monoprotonated at N7 (entries 2–6), diprotonated at N7 and N3 (entries 7–9) and not protonated (entry 1). Tables 5 and 6 show that monoprotonated guaninium cations connect together in two ways: either *via* only one relatively weak centrosymetric $R_2^2(8)$ N2···N3 hydrogen bond (entries 3 and 6) or *via* two strong hydrogen bonds, centrosymetric $R_2^2(8)$ N2···N3 and $R_2^2(10)$ N7···O6 (entries 2, 4 and 5). It is interesting to note that in guanine hydrobromide and hydrochloride monohydrate (entries 4 and 5, respectively) guaninium cations connect together in a similar fashion giving rise to the formation of perpendicular layers. In guanine hydrochloride dihydrate (entry 6) guaninium cations show a different type of interconnection, but they always form perpendicular layers. However, in the diprotonated cases guanine cations are not held together as seen in entries 8 and 9; in one case they are connected *via* only one strong hydrogen bond, N9···O6 (entry 7). In non-protonated guanine (entry 1), pairs of guanine bases are linked through three weak hydrogen bonds first *via* centrosymetric $R_2^2(8)$ N9···N3, secondly through N7···N1 and thirdly *via* N2···O6.

The monoprotonation of the guanine base at N7 shortens the C4—C5, C5—N7 and C8—N9 bonds by 0.0296, 0.0217 and 0.0238 Å, respectively (Fig. 12 – see supplementary material) and enlarges the C5—N7—C8 angle by 3.94°, while reducing the N7—C8—N9 angle by 3.66° (Fig. 12 – see supplementary

Table 5
CSD search on hybrid guanine salts.

Entry	Compound name and refcode as given in CSD	Chemical structure as given in CSD	Overall supramolecular network	Anion position†	Comment
1	Guanine monohydrate (GUANMH10)	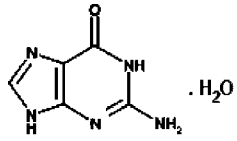	Three-dimensional	–	Water molecule makes a strong hydrogen bond with O6 and a weaker one with N2. Guaninium cations are related together in two ways: (i) *via* centrosymmetric N3···N9 hydrogen bonds and (ii) *via* O6···N2 and N7···N1.
2	Bisguaninium hydrogenphosphate hydrate (DUKKOJ)	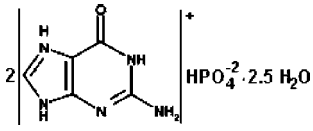	Three-dimensional	N9	Water molecule O*W*1 makes a hydrogen bond with N1 and the water molecule O*W*2 atom is not involved in hydrogen bonding. Guaninium cations are related in two ways: (i) *via* centrosymmetric $R_2^2(8)$ N3···N2 hydrogen bonds and (ii) *via* centrosymmetric $R_2^2(10)$ O6···N7. They also form layers parallel to the diagonal of the *ab* plane.
3	Guanine picrate monohydrate (GUNPIC10)	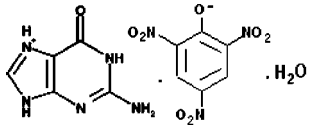	Three-dimensional	N9	Water molecule makes a hydrogen bond with N7 and O6. Guaninium cations are related by centrosymmetric $R_2^2(8)$ N3···N2 hydrogen bonds.
4	Guanine hydrobromide monohydrate (GUANBM)	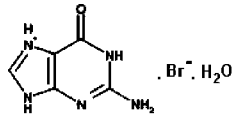	Three-dimensional	N9	Water molecule makes a hydrogen bond with N1. Guaninium cations are related in two ways: (i) *via* a centrosymetric $R_2^2(8)$ N3···N2 hydrogen bond and (ii) *via* centrosymetric $R_2^2(10)$ O6···N7 and form perpendicular layers.
5	Guanine hydrochloride monohydrate (GUANCH01)	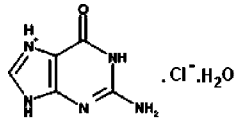	Three-dimensional	N9	Water molecule makes a hydrogen bond with N1. Guaninium cations are related in two ways: (i) *via* a centrosymetric $R_2^2(8)$ N3···N2 hydrogen bond and secondly *via* centrosymetric $R_2^2(10)$ O6···N7 and form perpendicular layers.
6	Guanine hydrochloride dihydrate (GUANCD)	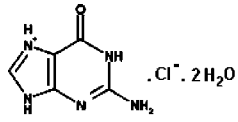	Three-dimensional	N1	Water molecule O1*W* atom makes a hydrogen bond with N7 and O2*W* makes a hydrogen bond with N9. Guaninium cations are related by a centrosymmetric $R_2^2(8)$ N3···N2 hydrogen bond and also form perpendicular layers.

† For atom numbering see Fig. 1.

material). The diprotonation of the guanine base at N7 and N3 increases the N3—C2 bond by 0.037 Å and reduces the N1—C2 bond by 0.0213 Å (Fig. 13 – see supplementary material). The C2—N3—C4 angle increases by 5.4°, while the N1—C2—N3 and N3—C4—C5 angles decrease by 4.99 and 4.06°, respectively (Fig. 13 – see supplementary material).

As seen from Tables 5 and 6, anions, *i.e.* proton donors interacting with guanine bases, are in most cases connected directly to the imino group N9 atom in the guanine monoprotonated salts and are connected to both the N9 and N3 atom imino groups in the diprotonated cases, whereas water molecules are observed to form strong hydrogen bonds with the imino group N7 atom. However, in compounds (I) and (III) studied here, the $H_2PO_3^-$ and $H_2PO_4^-$ anions are hydrogen bonded directly to the N7 imino group, whereas water molecules form strong hydrogen bonds with the imino group N9. This is the first case in which phosphate or phosphite anions are linked directly to the imino group N7 *via* a strong hydrogen bond in guaninium salts. This raises the question: Does protonation at N7 indicate that before protonation the N9H tautomer was the favored form? In fact, inspection of hydrogen bonding in all the compounds listed in Tables 5 and 6 revealed that the hydrogen bonds between the imino group N7 atom and the anions or water molecules appear to be shorter than those observed between the imino group N9 atom and the anions or water molecules. To confirm such a hypothesis, deuterated phosphorous acid should be used and a neutron diffraction experiment performed to follow the protonation process in these salts and to show definitively where the protonation occurs.

Table 6
CSD search on hybrid guanine salts and compounds studied here (continuation of Table 5).

Entry	Compound name and refcode as given in CSD	Chemical structure as given in CSD	Overall supramolecular network	Anion position	Comment
7	Guanine dihydrochloride (GODYUT)	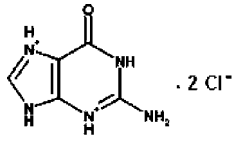	Two-dimensional	N3 and N9	Guaninium cations are related by only one strong O6···N9 hydrogen bond.
8	Guaninium dinitrate dihydrate (HUMNEI)	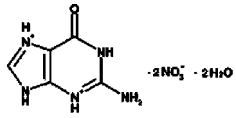	Two-dimensional	N3 and N9	Water molecule O1*W* atom makes a hydrogen bond with N7 and O2*W* makes a hydrogen bond with NO_2 groups. The two water molecules are connected by a strong hydrogen bond. Guaninium cations are not held together.
9	Guaninium sulfate monohydrate (HUSBEC)	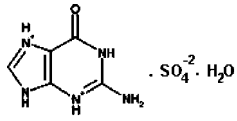	Three-dimensional	N3 and N9	Water molecule makes a hydrogen bond with N7 and O6. Guaninium cations are not held together.
(I)	Guaninium hydrogenphosphite monohydrate (this work)	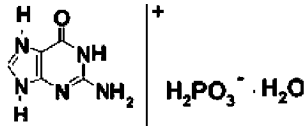	Three-dimensional	N7	Water molecule makes a strong hydrogen bond with N9 and guaninium cations are related by a centrosymetric $R_2^2(8)$ N3···N2 and form perpendicular layers.
(II)	Guaninium hydrogenphosphite dihydrate (this work)	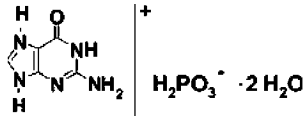	Three-dimensional	N9	Water molecule O*W*1 atom makes a strong hydrogen bond with N7 and O*W*2 makes a hydrogen bond with N1. Guaninium cations are related by centrosymetric $R_2^2(8)$ N3···N2.
(III)	Guaninium dihydrogenmonophosphate monohydrate (this work)	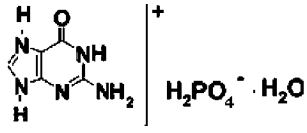	Three-dimensional	N7	Water molecule makes a strong hydrogen bond with N9 and guaninium cations are related by centrosymetric $R_2^2(8)$ N3···N2.

5. Conclusion

The crystal structures of the guaninium salts have been determinated and show different anion packing. Inspection of hydrogen bonding between the phosphite (phosphate) anion and the guanine cation shows, for the first time, a direct hydrogen-bond interaction between the guanine N7—H residue and OPO_2H (OPO_3H).

This is in favor of the N9H tautomeric form. A neutron diffraction experiment using deuterated phosphorous or phosphoric acid might help to confirm such a hypothesis. Further work in this direction is planned.

The authors would like to thank the service Commun de Diffraction X sur Monocristaux (Université Henri Poincaré, Nancy 1) for providing access to crystallographic experimental facilities. Authors are indebted to Professor Robert H. Blessing of the Hauptman–Woodward Medical Research Institute and the State University of New York at Buffalo, and to Professor B. Vitoux for many helpful discussions. We are also very grateful to A. Bouché and E. Wenger for expert technical assistance. E. Bendeif is grateful to l'Agence Universitaire de la Francophonie (AUF) for financial support (Imputation coda: 1021FR412L).

References

Allen, F. H. (2002). *Acta Cryst.* B**58**, 380–388.
Averbuch-Pouchot, M. T. (1993). *Acta Cryst.* C**49**, 815–818.
Barsky, D. & Colvin, M. E. (2000). *J. Phys. Chem. A*, **104**, 8570–8576.
Becker, E. D., Miles, H. T. & Bradley, R. B. (1965). *J. Am. Chem. Soc.* **87**, 5575–5582.
Bendeif, E. E. (2007). In preparation.
Bendeif, E. E., Dahaoui, S., Franccaronois, M., Benali-Cherif, N. & Lecomte, C. (2005). *Acta Cryst.* B**61**, 700–709.
Bernstein, J., Davis, R. E., Shimoni, L. & Chang, N. L. (1995). *Angew. Chem. Int. Ed. Engl.* **34**, 1555–1573.
Blessing, R. H. (1995). *Acta Cryst.* A**51**, 33–38.
Boukhris, A., Lecomte, C., Wyncke, B., Brehat, F. & Thalal, A. (1994). *J. Phys. Condens. Matter*, **6**, 2475–2490.

Broomhead, J. M. (1951). *Acta Cryst.* **4**, 92–99.
Brown, D. M. & Hewlins, M. J. E. (1968). *J. Chem. Soc.* pp. 2050–255.
Bugg, C. E. (1972). *In the Purines. Theory and Experiment*, edited by E. D. Bergmann & B. Pullman, pp. 178–204. Jerusalem: Academic Press.
Bugg, C. E. & Thewalt, U. (1975). *Acta Cryst.* B**31**, 121–127.
Chan, S. I. & Lee, G. C. Y. (1972). *Jerusalem Symp. Quant. Chem. Biochem.* **4**, 277.
Choi, M. Y. & Miller, R. E. (2006). *J. Am. Chem. Soc.* **128**, 7320–7328.
Cohen, B., Hare, P. M. & Kohler, B. (2003). *J. Am. Chem. Soc.* **125**, 13594–13601.
Colominas, C., Luque, F. J. & Orozco, M. (1996). *J. Am. Chem. Soc.* **118**, 6811–6821.
Del Bene, J. E. (1983). *J. Phys. Chem.* **87**, 267–371.
DeTitta, G. T. (1985). *J. Appl. Cryst.* **18**, 75–79.
Doran, M., Walker, S. M. & O'Hare, D. (2001). *Chem. Commun.* pp. 198–199.
Farrugia, L. J. (1997). *J. Appl. Cryst.* **30**, 565–566.
Farrugia, L. J. (1999). *J. Appl. Cryst.* **32**, 837–838.
Guille, K. & Clegg, W. (2006). *Acta Cryst.* C**62**, o515–o517.
Harrison, W. T. A. (2001). *J. Solid State Chem.* **160**, 4–7.
Harrison, W. T. A. (2003*a*). *Acta Cryst.* E**59**, o1267–o1269.
Harrison, W. T. A. (2003*b*). *Acta Cryst.* E**59**, o769–o770.
Iball, J. & Wilson, H. R. (1963). *Proc. R. Soc. London*, **288**, 418–429.
Katritzky, A. R. & Waring, A. J. (1963). *J. Chem. Soc.* pp. 3046–3051.
Kenner, G. W., Reese, C. B. & Todd, A. R. (1955). *J. Chem. Soc.* pp. 855–858.
Kokko, J. P., Mandell, L. & Goldstein, J. H. (1962). *J. Am. Chem. Soc.* **84**, 1042–1047.
Kwiatkowski, J. S. & Pullman, B. (1975). *Adv. Heterochem. Chem.* **18**, 199–327.
Lee, G. C. Y. & Chan, S. I. (1972). *J. Am. Chem. Soc.* **94**, 3218–3229.
Lee, G. C. Y., Prestegard, J. H. & Chan, S. I. (1971). *Biochem. Biophys. Res. Commun.* **43**, 435–439.
Lee, G. C. Y., Prestegard, J. H. & Chan, S. I. (1972). *J. Am. Chem. Soc.* **94**, 951–959.
Lin, J., Yu, C., Peng, S., Akiyama, I., Li, K., Lee, L. K. & LeBreton, P. R. (1980). *J. Phys. Chem.* **84**, 1006–1012.
Low, J. N., Tollin, P. & Young. D. W. (1986). *Acta Cryst.* C**42**, 1045–1047.
Maixner, J. & Zachová, J. (1991). *Acta Cryst.* C**47**, 2474–2476.
Masse, R. & Durif, A. (1990). *Z. Kristallogr.* **190**, 19–32.
Miles, H. T., Howard, F. B. & Frazier, J. (1963). *Science*, **142**, 1458–1463.
Oxford Diffraction (2004). *CrysAlis CCD* and *CrysAlis RED*. Oxford Diffraction Ltd, Abingdon, Oxfordshire, England.
Paixão, J. A., Matos Beja, A., Ramos Silva, M. & Martin-Gil, J. (2000). *Acta Cryst.* C**56**, 1132–1135.
Pecaut, J. & Bagieu-Beucher, M. (1993). *Acta Cryst.* C**49**, 834–837.
Schweizer, M. P. & Hollis, D. P. (1969). *Ann. N. Y. Acad. Sci.* **158**, 256–297.
Shapiro, R. (1968). *Prog. Nucl. Acid Res. Mol. Biol.* **8**, 73–112.
Sheldrick, G. M. (1997). *SHELXS*97 and *SHELXL*97, Release 97–2. University of Göttingen, Germany.
Slósarek, G., Kozak, M., Gierszewski, J. & Pietraszko, A. (2006). *Acta Cryst.* B**62**, 102–108.
Spek, A. L. (2003). *J. Appl. Cryst.* **36**, 7–13.
Taylor, R. & Kennard, O. (1982). *J. Mol. Struct.* **78**, 1–28.
Thewalt, U., Bugg, C. E. & Marsh, R. E. (1971). *Acta Cryst.* B**27**, 2358–2363.
Topal, M. D. & Fresco, J. R. (1976). *Nature*, **263**, 285–289.
Watson, J. D. & Crick, F. H. C. (1953). *Nature (London)*, **171**, 737–738.
Wolfenden, R. V. (1969). *J. Mol. Biol.* **40**, 307–310.
Wong, Y. P. (1973). *J. Am. Chem. Soc.* **95**, 3511–3515.
Yun, H. J., William, A. G., Katherine, T. N., Lawrence, C. S., Sungu, H. & Doo, S. C. (2003). *J. Phys. Chem. B*, **107**, 344–357.